

# Atomic structure and work function of metal-film system lithium + (011) face of tungsten or molybdenum

O. V. Kanash and A. G. Fedorus

*Physics Institute, Ukrainian Academy of Sciences*

(Submitted 18 May 1983)

*Zh. Eksp. Teor. Fiz.* **86**, 223–231 (January 1984)

The LEED method and the contact-potential difference method are used to study the atomic structure and phase transitions in lithium films, as well as the change of the work function when lithium is absorbed on the (011) face of W or Mo in a wide range of submonolayer coverages. At low coverage ( $\vartheta < 5/9$ ) the structures produced on these substrates are characterized by a rather isotropic distribution of the adatoms over the surface. At high coverage ( $\vartheta > 5/9$ ) identical sequences of anisotropic structures, indicative of localized adsorption, are produced on both substrates. In the region of  $\vartheta$  from 1/4 on W(011) and 1/6 on Mo(011) to 5/9 (on both substrates) the film grows via successive first-order phase transitions. In the remaining regions of the film compression proceeds continuously. To explain the continuity of the film compression, a model of mixing of cells of unequal size is used. The character of the film structure corresponds to a predominant influence of dipole–dipole interaction between the adatoms at low coverage and to continuous interaction at high coverage. The thermal stability of the films at different  $\vartheta$  is investigated. The influence of the film structure on the work function and on the surface diffusion is investigated.

## INTRODUCTION

A feature of the atomic structure of submonolayer films of electropositive elements adsorbed on atomically smooth faces of metallic crystals is the isotropic distribution of the adatoms and the formation of two-dimensional lattices with large periods during the early film-growth stages, and of hexagonal lattice when a monolayer is approached. This is due to the dipole–dipole interaction of the adatoms (which is isotropic, repulsive, and long-range), which predominates in systems of this type. The lithium adatom, however, has a small dipole moment  $p$  compared with other electropositive adsorbates (its initial value on W(011) is  $p = 2.3$  D and decreases with increasing degree of coverage to  $p < 1$  D (Ref. 1); it is therefore to be expected that the indirect interaction of the lithium atoms (which are anisotropic and oscillatory in space) likewise plays an important role in the formation of the film structure.<sup>2,3</sup> Data on the structure of Li films on W(011), obtained by the LEED method, are given in two papers.<sup>4,5</sup> In Ref. 5 was reported observation of sufficiently isotropic structures ( $3 \times 2$ ),  $c(2 \times 2)$  and  $c(1 \times 3)$  at low coverages  $\vartheta$  equal to 1/6, 1/4, and 1/3, respectively. The value  $\vartheta = 1$  corresponds to a lithium density in the monolayer ( $n = 1.4 \cdot 10^{15} \text{ cm}^{-2}$ ) which was found<sup>5</sup> to duplicate the substrate structure. For large coverage, anisotropic-structure models were proposed in the form of close-packed rows of adatoms that duplicate the substrate structure along  $\langle 100 \rangle$ , with the distance between the rows determined by the degree of coverage. The presence of such rows is evidence of the important role of the indirect interaction.

The complicated nature of the forces acting between the Li adatoms manifests itself in the phase transitions that occur when  $\vartheta$  is varied. For example, on W(011) in the region  $\vartheta = 1/4$ – $1/3$  there coexist two phases,  $c(2 \times 2)$  and  $c(1 \times 3)$ ,<sup>5</sup> i.e., a first-order phase transition takes place. The phase transitions exert a strong influence on a number of surface

phenomena, particularly on the character of the change of the work function and on the surface diffusion parameters. In the first-order phase transition region the work function is linear in  $\vartheta$  (Ref. 6) and the diffusion activation energy increases according to Refs. 7 and 8.

The main task of the present study was therefore to obtain the possibly most complete picture of the changes in the atomic structure of lithium films for submonolayer coatings on the (011) face of tungsten or molybdenum, with an aim of shedding light on the variation of the character of the interaction of lithium adatoms with changing  $\vartheta$ . Another task was a detailed investigation of the phase transitions in these systems for the purpose of further study of their influence on the film properties.

## EXPERIMENT

The atomic structure of lithium films was investigated by the LEED method using glass devices in which the samples could be heated to  $T = 2400$  K and cooled with liquified gas (usually nitrogen). The construction of the device used to study the Li–W(011) system made possible cooling the sample with liquid helium.<sup>9</sup> The intensity of the LEED reflections was measured with a telescopic photometer. The work function was measured by the contact-potential-difference method, using either the LEED electron gun or a three-electrode gun that could be moved close to the crystal. The details of the experimental procedure (including temperature measurements, determination of the coverage, the decrease of the effect of the electron-stimulated disorder on the measurement of the LEED reflection intensity), as well as the sample preparation, are described in Refs. 6 and 9. A high-purity atomic lithium beam was produced by an evaporator designed by Gavriilyuk and Medvedev.<sup>10</sup> The films were evaporated in measured batches, after which they were annealed when necessary. Annealing to  $T = 70$ – $100$  K was

needed to obtain a sufficiently perfect structure at low coverage ( $\vartheta \leq 1/3$ ), and to a temperature closer to the desorption temperature at larger coverage (e.g., to 600 K at  $\vartheta = 2/3$ ). Growing films with as perfect a structure as possible was particularly important for the Li-Mo(011) system, for in this case the lithium surface density was determined only from structure-analysis data under the assumption that a maximum of the work function vs coverage corresponds to a closely packed monolayer. The results in this case were then in agreement for different coverages. For the Li-W(011) system the graduation of the surface density of the adatoms was additionally monitored against the known<sup>10</sup> density dependence of the work function.

For W(011) we investigated the structure of films in thermal equilibrium (annealed) as well as of those not in equilibrium (evaporated directly on a substrate cooled to  $T = 5$  K). In nonequilibrium films there is no long-range order in the entire submonolayer region, but there are certain short-range order forms, as attested by the anisotropy of the scattering intensity on the LEED patterns (Figs. 1a, 1b).

At  $\vartheta < 1/9$  the structure cannot be made perfect by annealing. It appears that at large distances between adatoms their interaction is weak and the order-disorder transition temperature does not exceed the temperature at which the adatoms have noticeable mobility, so that the so-called chaotic phases, characterized by LEED patterns with smeared

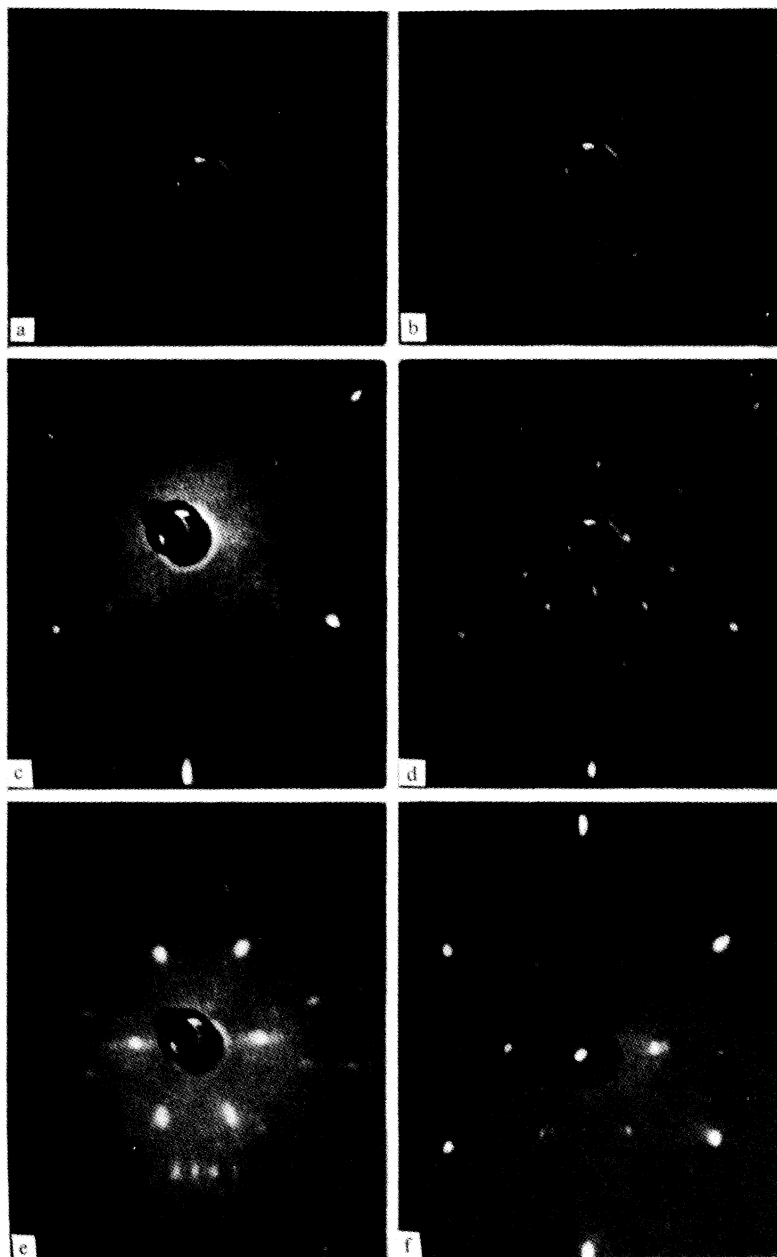


FIG. 1. Electron-diffraction patterns: (a-e) for films Li-W(011),  $T = 5$  K (a, b) not annealed, (c-e) annealed at 300 K; f) for films Li-Mo(011),  $T = 77$  K (annealed at 250 K). Coverage and electron energy (eV): a)  $- 1/8$  and 17 (at this energy one cannot see the substrate reflections, only the surrounding specular reflection); b)  $- 2/3$ , 17; c)  $- 1/20$ , 40; d)  $- 1/8$ , 40; e)  $- 4/9$ , 26 (only the film reflections are seen); f)  $- 9/28$ , 76.

reflections, can set in (Fig. 1c).

The first well-ordered structures in annealed films appear at sufficiently low  $T$  in the vicinity of  $\vartheta = 1/8$  (Fig. 1d). With increasing  $\vartheta$  the additional reflections move continuously away from the main ones. At values  $\vartheta = 1/8, 1/6,$  and  $1/4$  the diffraction patterns of the commensurate structures  $c(2 \times 4), (3 \times 2)_2$  and  $c(2 \times 2)$  are observed. Just as the centered cells labeled "c," the  $(3 \times 2)_2$  cell is not primitive, and to designate the number of adatoms in it we shall use here and elsewhere a numerical subscript. In the region  $\vartheta = 1/4 - 1/3$  one can see a picture of the LEED patterns corresponding to the  $c(2 \times 2)$  and  $c(1 \times 3)$  lattices, while in the region  $\vartheta = 1/3 - 5/9$  there is also superposition of LEED patterns corresponding to two structures (Fig. 1e); the first is  $c(1 \times 3)$  as before, possibly shrunk somewhat because of admixture of denser cells (the electron-diffraction pattern shows satellites in addition to the  $c(1 \times 3)$  reflections), while the second is tentatively designated  $(3 \times 1)^*$  and its model will be discussed below. Figure 2a shows the intensity variation of the reflections  $(3 \times 2)_2, c(2 \times 2)$  and  $c(1 \times 3)$  as functions of the coverage  $I(\vartheta)$ . The horizontal rows of the  $(3 \times 1)^*$  reflections that remain after the  $c(1 \times 3)$  reflections vanish at  $\vartheta = 5/9$  merge into single reflection as  $\vartheta$  increases further from  $5/9$  to  $2/3$ . The latter reflections shift into positions corresponding to the structure  $(3 \times 1)_4$ , so that the electron diffraction pattern takes the form described in Ref. 4. The increase of  $\vartheta$  in the sequence  $2/3, 3/4, 4/5, 5/6,$  etc., to 1 leads to the appearance of the LEED patterns described in Ref. 4 (the additional reflections divide the distance between the principal ones along the  $\langle 0\bar{1}1 \rangle$  axis into an integer number of parts), except that in Ref. 4 the values  $\vartheta = 1/3, 1/2, 3/5, 3/$

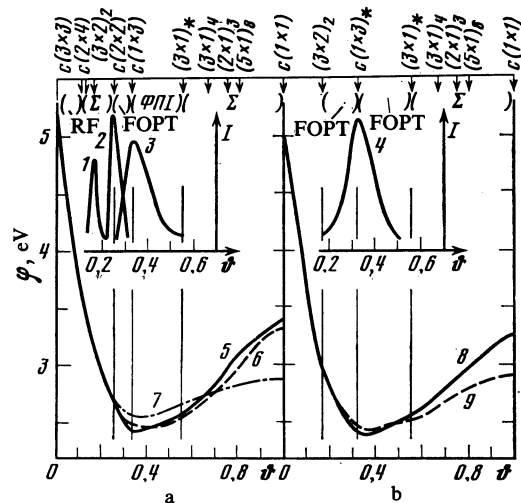


FIG. 2. Intensity of reflections of film  $I$  (1-4) and work function  $\varphi$  (5-9) vs the coverage  $\vartheta$ , and also schemes of structural transitions of submonolayer lithium films adsorbed on the (011) surface of tungsten (a) and molybdenum (b). Curves 1-3) for respective reflection of annealed films  $(3 \times 2)_2, c(2 \times 2)$  and  $c(1 \times 3)$ ,  $T = 5$  K; 4) for  $c(1 \times 3)$ ,  $T = 77$  K; 7, 9) for non-annealed films adsorbed at 5 and 77 K, respectively; 5, 6, 8) for annealed films at  $T = 5, 300,$  and  $77$  K, respectively. (RF)—random phases, ( $\Sigma$ )—structures of the cell-mixture type, (FOPT)—first-order phase transition; the boundaries of the FOPT regions are marked by vertical lines; the arrows indicate the stoichiometric values of  $\vartheta$  for the corresponding structures.

2, and  $3/1$  were determined for them. The causes of the disparity can be either the ambiguity in the possible interpretation of the electron-diffraction patterns or the absence, at room temperature, of ordered structures of a different type that might be used to determine the adatom density. At  $\vartheta = 1$  all the additional reflections vanish; the films structure apparently duplicates the substrate structure.

The thermal stability of the described structures increases with increasing degree of coverage. At  $\vartheta \leq 1/3$  it was investigated in Refs. 5 and 12; we recall that the disorder sets in below room temperature (100-235 K). We note that at  $\vartheta = 1/8 - 1/4$  the diffraction patterns observed for thermally disordered films do not differ from those obtained for non-equilibrium (non-annealed) films at the same coverages. In the  $(3 \times 1)^*$  structure and in the transition region  $\vartheta = 5/9 - 2/3$  the order is also preserved only at low temperatures ( $\leq 200$  K). The  $(3 \times 1)_4$  structure is the first ordered structure that exists below room temperature. In the region  $\vartheta \gg 2/3$  the influence of the temperature on the character of the order has the following feature. In well-annealed films the additional reflections have an oval shape at the exact values  $\vartheta = 2/3, 3/4, 4/5,$  etc. If  $T \geq 200$  K their shape remains the same also at intermediate values of  $\vartheta$ , and with changing  $\vartheta$  they are continuously shifted. But if  $T$  is lowered, one-dimensional splitting appears at intermediate  $\vartheta$  and the indicated reflections are broadened along  $\langle 0\bar{1}1 \rangle$ .

The experiments on Mo(011) were performed at  $T \geq 77$  K. At liquid-nitrogen temperature the film becomes well ordered at coverages  $1/6 - 5/9$  without additional annealing. In this rather wide range of coatings, two superpositions of the LEED patterns are observed in succession, each consisting of a pair of reflection systems. One of these systems, which contains both pairs, is shown in Fig. 1f, and the model of its corresponding structure, designated for the time being  $c(1 \times 3)^*$ , will be discussed later. It is observed in the entire range  $\vartheta = 1/6 - 5/9$  (the  $I/\vartheta$  dependence is shown in Fig. 2.4): first, at  $\vartheta = 1/6 - 9/28$ , together with the strongly smeared and weakened picture of the  $(3 \times 2)_2$  structure whose brightness decreases with increasing  $\vartheta$ , and then, at  $\vartheta = 9/28 - 5/9$ , together with the pattern of the  $(3 \times 1)^*$  structure (the same as for Li-W(011) in the  $\vartheta = 1/3 - 5/9$  region), and its brightness increases with  $\vartheta$ .

At  $\vartheta > 5/9$  the structure of the lithium films on Mo(011) is the same as on W(011).

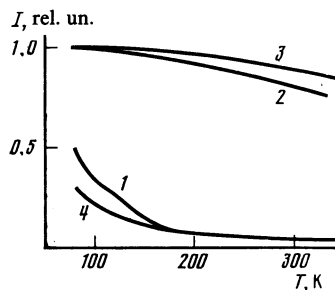


FIG. 3. Temperature dependence of the intensity of the reflections of lithium films adsorbed on 1)  $c(1 \times 3)^*$ ; 2)  $(3 \times 1)_4$ ; 3)  $(2 \times 1)_3$ . Also shown is curve 4 for three-dimensional lithium crystals growing on top of the  $c(1 \times 1)$  coating.

Figure 3 shows the temperature dependences of the intensity of the additional reflections for the basic structures of Li films on Mo(011); these dependences are indicative of the thermal stability of these structures. Just as in the case of Li adsorption on W(011), the ordering of the films at low coverages ( $\vartheta < 5/9$ ) sets in after substantial cooling. Thus, even the liquid-nitrogen temperature is insufficient to order films with  $\vartheta = 9/28$ . The structure of denser films ( $\vartheta > 2/3$ ) is stable almost up to the desorption temperature.

Figure 2 shows the dependences of the work function  $\varphi(\vartheta)$  on the coverage obtained for lithium films under various adsorption and annealing systems. The minimum of the  $\varphi(\vartheta)$  curve for the Li-W(011) system corresponds to a structure  $c(1 \times 3)$  with an adatom density  $n = 4.7 \cdot 10^{14} \text{ cm}^{-2}$ , in good agreement with the density measured by the quartz microbalance method.<sup>10</sup> At  $T = 5 \text{ K}$  the values of  $\varphi$  obtained at the minimum and at other points, obtained for annealed films, do not differ from the data given in Refs. 7 and 13 for  $T = 77 \text{ K}$ .

## DISCUSSION OF RESULTS

At low degrees of coverage ( $\vartheta < 1/3$ ) the structures produced have an isotropic adatom distribution and large lattice periods. The formation of such structures attests to the decisive role played in this process by dipole-dipole interaction between the adatoms. These structures include all the commensurate centered structures obtained for the Li-W(011) system, as well as the  $(3 \times 2)_2$  lattice observed for both systems, as well as the  $(3 \times 2)_2$  lattice observed for both systems. Most of these commensurate structures exist in narrow coating ranges that correspond to their stoichiometry, as is shown by the sharp peaks on the  $I(\vartheta)$  plot, e.g., in the  $\vartheta = 1/6$  region (Fig. 2, curve 1). At intermediate values of  $\vartheta$  the film structure can no longer be made up of identical primitive cells under the assumption that the adsorption is localized, i.e., with all the adatoms located at the substrate lattice sites (in structures of the lattice type). A transition to an incommensurate phase is not very likely because of the relatively deep potential relief of the substrate ( $\sim 0.1 \text{ eV}$ , Ref. 7). The continuity of the process of film compression with increasing  $\vartheta$ , and the corresponding observed continuity of the shift of the additional reflections in this case, can be explained on the basis of the model previously proposed<sup>14</sup> for the Sr-W(011) system, with mixing of cells that are close in size ( $\Sigma$  structures). That this structure is defective is revealed by the considerable decrease of the intensity and by the broadening of the reflections, which is observed, e.g., on going from  $\vartheta = 1/6$  to  $\vartheta = 1/4$  (Fig. 2, curves 1 and 2). At large lattice periods, however, the broadening is smaller than the instrumental broadening<sup>15</sup> and is therefore not observed at small  $\vartheta$ .

When lithium was adsorbed on Mo(011), the  $c(1 \times 3)^*$  structure, not encountered previously, was observed in the region of small besides  $c(3 \times 2)_2$ . The additional reflections are located on the electron-diffraction pattern (Fig. 1f) at about the same places as for the known structure  $c(1 \times 3)$ , but they are split into doublets of unequal intensity. The splitting of the reflections on the electron diffraction pattern is reminiscent of the pattern obtained for antiphase domains.<sup>16</sup> For

its interpretation we calculated in the kinematic approximation the domain structure factor of the  $c(1 \times 3)$  structure as a nonprimitive cell with different displacement vectors on a domain wall passing parallel to the  $\langle 011 \rangle$  axis. Figure 4a shows for the  $c(1 \times 3)$  structure a model that satisfies best, in accord with the results of the calculation of the structure factor, the electron-diffraction singularities described above. The corresponding value  $\vartheta = 9/28$  agrees well with the experimental value at which  $I(\vartheta)$  goes through a maximum. In contrast to antiphase domains, on the wall between which the displacement vector is half the film lattice period, here it is equal to  $2/3$  of the  $c(1 \times 3)$  lattice period, and it is this which causes the different intensities of the doublet components.

Obviously, the formation of domains with disordered walls is due to the mismatch of the film and substrate structures. Thus, assuming dipole-dipole interaction between the adatoms, one might expect the film to have an isotropic hexagonal configuration that is not commensurate with the slightly elongated triangular structure of the substrate. In this case, however, the displacement on the domain wall increases rather than decreases the anisotropy of the film structure. The dipole-dipole interaction can therefore hardly play any role in the formation of domain walls such as in Fig. 4a. Judging from the anisotropy and long-range action of the factor that leads to the onset of domains, indirect interaction should play the major role. Additional proof in favor of this assumption is the appearance of the  $c(1 \times 3)^*$  phase in the form of islands, which can be regarded as a manifestation of the spatially oscillatory character of the interaction between the adatoms. Thus, besides the features typical of dipole-dipole interaction, features of indirect interaction appear in the atomic structure of a lithium film on Mo(011) in the region  $\vartheta \approx 1/3$ .

The geometry of the electron diffraction patterns observed for both substrates at large coverages ( $\vartheta \geq 2/3$ ), namely the absence of additional reflections on the lines joining the main reflections along the  $\langle 100 \rangle$  axis, leads to the unam-

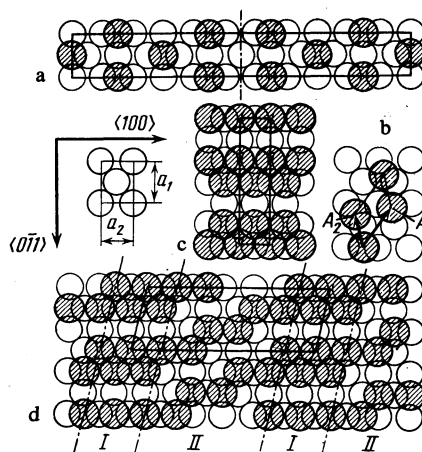


FIG. 4. Structure models: a)  $c(1 \times 3)^*$ ; b)  $(3 \times 1)_4$ ; c, d) incommensurate and lattice structures at  $\vartheta = 5/9$ .  $A_1$  and  $A_2$  are the translation vectors of the incommensurate cell. On the left is shown the substrate  $c(1 \times 1)$  structure cell with periods  $a_1$  and  $a_2$ . The shaded circles designate adatoms.

biguous conclusion that the structure of the film comprises a set of rows parallel to the  $\langle 100 \rangle$  axis, in which the adatoms are packed almost flush one against the other and duplicate the sequence of the substrate surface atoms. The average distance between the rows along the  $\langle 0\bar{1}1 \rangle$  axis direction cannot be established unambiguously from the form of the electron diffraction pattern, and is determined for each structure, as mentioned above, with account taken of the data on the coating data obtained either independently<sup>10</sup> or in accord with other structures for the same system. An important role in the choice of the structure model, however, is played also by the question of whether these rows are equally spaced or whether their distribution is affected by the substrate potential relief. The fact that the adatoms duplicate along the row the periodicity of the substrate is evidence in favor of the premise that the adsorption of the lithium in this coverage range is localized. A more acceptable model of the film structure is therefore the lattice model, in which the substrate relief is followed not only by the adatoms in each row, but also by the row itself, while the average distance between the rows is maintained equal to  $1/\vartheta$  of the distance between the rows, owing to the presence of a structure with more or less equally spaced vacant rows. Thus, in the  $(3 \times 1)_4$  structure at  $\vartheta = 2/3$  (Fig. 4b), two rows of adatoms alternate with one vacant row, while in the structure  $(2 \times 1)_3$  at  $\vartheta = 3/4$  three rows of adatoms alternate with one vacant row, etc. The range of the effective mutual repulsion of the vacant rows is rather long: after a thorough annealing it was possible to obtain structures of vacant rows with periods up to nine inter-row distances of the substrate. Even larger periods were recorded in their substructures observed at  $T < 200$  K.

The electron-diffraction pattern of the  $c(1 \times 3)$  structure at  $\vartheta = 5/9$  (Fig. 1e), which precedes the formation of the rows along the  $\langle 100 \rangle$  axis, can also be ambiguously interpreted. Similar diffraction patterns were observed earlier for the Pb-W(011) system, and incommensurate-structure models were proposed for them.<sup>17</sup> Figure 5 illustrates the principle underlying the choice of the reciprocal-lattice cell by starting from the arrangement of the reflections on the electron-diffraction pattern (Fig. 1e) and with account taken of the experimentally established value  $\vartheta \approx 0.55$ . Figure 4c shows the corresponding cell of the incommensurate adatom structure. An electron diffraction pattern of the same geometry, however, is obtained also for the lattice structure in the form of domains with ordered walls (Fig. 4d). Calculation of the structure factor of the nonprimitive cell of this structure has shown its intense reflections to be in the same positions as the complete system of reflections, including satellites from multiple scattering) of the incommensurate film whose model is shown in Fig. 4c. In the structure shown in Fig. 4d it is possible to separate bands (I) that consist of  $(3 \times 1)_4$  cells and alternate with bands (II) of less dense cells (with local  $\vartheta = 1/2$ ). The mutual approach of the additional reflections as  $\vartheta$  is varied from  $5/9$  to  $2/3$  can be interpreted as a decrease of the width of the bands (II), until they are completely crowded out. We emphasize that this is not a first-order transition, since the film is macroscopically homogeneous. In the region  $\vartheta = 5/9 - 2/3$  the proposed lattice models agree better as  $\vartheta \rightarrow 2/3$  with the row model than incommen-

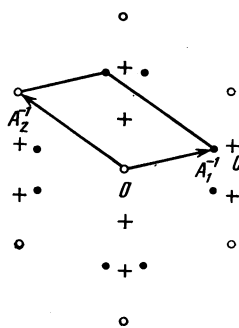


FIG. 5. Arrangement of LEED reflections at  $\vartheta = 5/9$ . Light circles—reflections of substrate, dark—of film, the crosses mark the positions of the  $(3 \times 1)_4$  reflections at which are merged additional reflections that move along the symmetry-axis line as  $\vartheta \rightarrow 2/3$ ;  $A_1^{-1}$  and  $A_2^{-1}$  are the reciprocal-lattice vectors for the incommensurate structure cell.

surate-structure model, and the former should therefore be given preference.

At  $\vartheta > 5/9$  the adatom density is already high enough to be able to realize within the scope of the lattice-structure model an isotropic adatom distribution such that they are more or less equidistant. In this case, however, the tendency of the adatoms to repel one another, should manifest itself at the onset of an isotropic vacancy structure, for example  $c(1 \times 3)_4$  at  $\vartheta = 3/2$ , and the symmetric adatom structure  $c(1 \times 3)$  at  $\vartheta = 1/3$ . Instead, noticeably anisotropic row structures along the  $\langle 100 \rangle$  axis are produced. The formation of anisotropic structures is evidence of an increased role of indirect interaction compared with the dipole-dipole interaction on going over to larger lithium coverage.

In Fig. 2 are summarized, in the form of structure-transition schemes, the proposed models of the low-temperature structures of annealed films. The coverage regions  $1/4 - 1/3$ ,  $1/3 - 5/9$  on W(011) and  $1/6 - 9/28$ ,  $9/28 - 5/9$  on Mo(011) are two-phase, and the film grows in them via a first order phase transition (FOPT). This is also in agreement with the linear variation of  $\varphi(\vartheta)$  in the indicated region. In the remaining range of  $\vartheta$  the submonolayer films are single-phase. A number of  $\varphi(\vartheta)$  features that are distinctly observed in experiments on Li-W(011) with temperature variation confirm the earlier conclusion that short-range rather than long-range order influences the work function.<sup>18</sup> These include the noticeable change of  $\varphi$  on melting of a two-phase film, as well as on annealing of dense coatings ( $\vartheta > 2/3$ ). In these cases the change of  $\varphi$  is observed either when the short-range order change, or on going from a random distribution to an ordered one.

In light of the singularities of the structure of Li films on W(011), let us examine the behavior of certain surface-diffusion parameters measured in Ref. 7. We recall that the surface-diffusion coefficient in the submonolayer region of  $\vartheta$  goes through a number of maxima, two of which are due to first-order transitions at  $\vartheta = 1/2$  and  $5/9$ . A similar correlation was observed earlier also for the Ba-Mo(011) system.<sup>6</sup> Thus, the presence of a maximum of  $D(\vartheta)$  and the linearity of  $\varphi(\vartheta)$  point to a possible first-order transition. The causes of the increased mobility of the adatom layer in the region of the first-order transition was discussed earlier.<sup>6</sup> The maxi-

mum of  $D(\vartheta)$ , however, can have also other causes: thus, two maxima were observed also in the single-phase region  $0.1 < \vartheta < 0.25$  ( $\Sigma$  structures).<sup>7</sup> A maximum of  $D(\vartheta)$  is therefore not a sufficient indication of a first-order transition.

In the entire submonolayer region, the structure of the lithium films on both substrates can be represented by lattice-type models. In this respect these films have an unusual behavior compared with other electropositive adsorbates, for which incommensurate hexagonal structures were observed at large coverages. Both the localized character of the adsorption and the manifestation of the indirect interaction in the anisotropy of the film structure at  $\vartheta > 5/9$  are apparently due to the small dipole moment of the Li adatoms. Since, however, the indirect interaction falls off on the (011) face like  $R^{-5}$  (Ref. 3), and the dipole-dipole interaction like  $R^{-3}$ , at large distances (at small  $\vartheta$ ) the second predominates nonetheless, and at short distances (large  $\vartheta$ ), the first. For the systems investigated, the largest distance on which a predominantly indirect interaction is observed is approximately two substrate periods (obtained as the averaged period of the film in the  $c(1 \times 3)^*$  structure of Li-Mo(011), see Fig. 4a). It is probable that the first-order transitions observed in extensive regions of  $\vartheta$ , within which effective attraction forces act between the adatoms, are also due to indirect interaction. On furrowed (112) faces of W and Mo, the indirect interaction of the adatoms gives rise to modulations with a period on the order of several substrate lattice constants, which are different on W and Mo.<sup>19</sup> In lithium films on the (011) faces of W and Mo the indirect interaction becomes the decisive factor in the formation of the structure only at substantially shorter distances between the adatoms, which are unfavorable for the observation of modulations of this kind. However, even at small coverage the indirect interaction apparently influences the film structure. Arguments in the favor of this statement were already presented above in the discussion of the  $c(1 \times 3)^*$  structure. In addition, the difference between the structures of the lithium films on the substrates, which are practically the same from the point of structure, is evidence that the interaction between the adatoms is not pure dipole-dipole.

Thus, when adsorbed on the (011) face of W or Mo, lithium behaves as an intermediate adsorbate, which exhibits at small coverage symptoms of the predominately ionic bonding inherent in other electropositive elements. At large coverage the bond is metallic and the lithium comes closer to adsorbates that have physical and chemical properties similar to those of the substrate.

The authors thank V. K. Medvedev for supplying the lithium source and A. G. Naumovets for a helpful discussion of questions of surface diffusion.

<sup>1</sup>E. V. Klimenko and A. G. Naumovets, *Fiz. Tverd. Tela (Leningrad)* **13**, 33 (1971) [*Sov. Phys. Solid State* **13**, 25 (1971)].

<sup>2</sup>T. B. Grimley, *Proc. Phys. Soc.* **90**, 751 (1967).

<sup>3</sup>O. M. Braun, *Fiz. Tverd. Tela (Leningrad)* **23**, 2779 (1981) [*Sov. Phys. Solid State* **23**, 1626 (1981)].

<sup>4</sup>D. A. Gorodetskii, Yu. P. Mel'nik, and A. A. Yas'ko, *Ukr. Fiz. Zh.* **12**, 649 (1967)].

<sup>5</sup>A. G. Naumovets and A. G. Fedorus, *Zh. Eksp. Teor. Fiz.* **68**, 1183 (1975) [*Sov. Phys. JETP* **41**, 587 (1975)].

<sup>6</sup>A. G. Fedorus, A. G. Naumovets, and Yu. S. Vedula, *Phys. stat. sol. (a)* **13**, 445 (1972).

<sup>7</sup>A. T. Loburets, A. G. Naumovets, and Yu. S. Vedula, *Surf. Sci.* **120**, 347 (1982).

<sup>8</sup>Yu. S. Vedula, A. T. Loburets, and A. G. Naumovets, *Zh. Eksp. Teor. Fiz.* **77**, 773 (1979) [*Sov. Phys. JETP* **50**, 391 (1979)].

<sup>9</sup>I. F. Lyuksyutov and A. G. Fedorus, *ibid.* **80**, 2511 (1981) [**53**, 1317 (1981)].

<sup>10</sup>V. M. Gavriilyuk and V. K. Medvedev, *Fiz. Tverd. Tela (Leningrad)* **8**, 1811 (1966) [*Sov. Phys. Solid State* **8**, 1439 (1966)].

<sup>11</sup>P. Bak, *Rep. Progr. Phys.* **45**, 587 (1982).

<sup>12</sup>A. G. Naumovets and A. G. Fedorus, *Zh. Eksp. Teor. Fiz.* **73**, 1085 (1977) [*Sov. Phys. JETP* **46**, 575 (1977)].

<sup>13</sup>V. K. Medvedev and T. P. Smereka, *Fiz. Tverd. Tela (Leningrad)* **16**, 1599 (1974) [*Sov. Phys. Solid State* **16**, 1046 (1974)].

<sup>14</sup>O. V. Kanash, A. G. Naumovets, and A. G. Fedorus, *Zh. Eksp. Teor. Fiz.* **67**, 1818 (1974) [*Sov. Phys. JETP* **40**, 903 (1974)].

<sup>15</sup>J. E. Houston and R. L. Park, *Surf. Sci.* **21**, 209 (1970).

<sup>16</sup>P. J. Estrum and E. G. McRae, *Surf. Sci.* **25**, 1 (1971).

<sup>17</sup>E. Bauer and H. Poppa, *Thin Solid Films* **28**, 19 (1975).

<sup>18</sup>A. G. Fedorus and A. G. Naumovets, *Surf. Sci.* **93**, L98 (1980).

<sup>19</sup>V. K. Medvedev, *Acta Univ. Wratisl.* **33**, 45 (1979).

<sup>20</sup>Yu. S. Vedula, V. V. Gonchar, A. G. Naumovets, and A. G. Fedorus, *Fiz. Tverd. Tela (Leningrad)* **19**, 1569 (1977) [*Sov. Phys. Solid State* **19**, 916 (1977)].

Translated by J. G. Adashko